FATIGUE CRACK GROWTH IN WELDED GIRDERS

O.I. Eide*, S. Berge+

Large scale welded girders with 20 mm plate thickness were tested in four point bending. Fatigue cracks which initiated at stiffeners welded to the web were monitored using high frequency potential drop techniques. Fatigue crack growth was analyzed for the various cracks on the basis of detailed stress analysis of the welds. The experimental data for individual crack locations could be unified on a curve which was in good agreement with the fracture mechanics analysis of crack growth. The model facilitates calculation of residual fatigue life and assessment of reliability of steel plated structures with crack-like defect.

INTRODUCTION

Current fatigue design codes and recommendations for steel plated structures (1-3) are based on S-N curves which have been derived from test data, in general from small scale uniaxial specimens, following the procedure of Gurney and Maddox (4). These S-N curves are to be applied under the condition that the structure complies with normal production standards.

In cases when cracks or weld defects have been detected, fracture mechanics may be used in residual fatigue life assessments, and for the evaluation of structural reliability, fracture toughness requirements, and inspection/repair criteria. Elements of such analyses have been demonstrated by Smith et al. (5) for the deck structure of a tension leg platform (TLP).

* Dr.ing., SINTEF, Trondheim, Norway
+ Prof., Div. of Marine Structures, The Norwegian Inst. of Technology, Trondheim, Norway

In order to check the accuracy of fracture mechanics crack growth analysis, two large scale welded girders with plate thickness 20 mm were tested.

The S-N data obtained with the models has been reported elsewhere (6, 7). The emphasis in the present paper is on fatigue crack growth, residual life assessment, and in-service inspection criteria.

EXPERIMENTAL INVESTIGATION

Specimen

The specimen was designed to comply with the following requirements,

- fatigue capacity less than 2000 kN load range
- size and method of fabrication which would give residual stresses and distortions relevant to large-scale structural members
- crack initiation and growth as in realistic structural welds

The large-scale plate girder with attachment welds shown in Fig. 1 was found to comply with these requirements. In addition, this type of specimen has been tested in a smaller scale in other laboratories, so that some background material exists (8-9).

The material used was a structural steel to OX 520D, generally conforming to the DnV standard for controlled yield strength steels (3). The yield strength was in the range 360-400 MPa.

Two plate girders were produced according to standard fabrication techniques. The web to flange fillet welds were made by the submerged-arc process. The stiffener fillet welds were produced by manual welding in the horizontal position using basic electrodes. The nominal weld throat was 30 per cent of the plate thickness. No post weld treatment was applied.

The specimens were tested in a four point bending fixture, employing two servohydraulic actuators in simultaneous computer control. The test rig arrangement is shown in Fig. 2. The specimens [1] - [2] were mounted in a specially designed steel frame rig [3], which allowed longitudinal displacements at the strong floor [4]. The specimens were simply supported at both

ends. At the middle of the plate girders, bearings [5] - [6] were mounted at the flanges in order to eliminate out-of-plane displacements. The actuators [7] - [8] were mounted in between the specimens, simply supported at the compression flanges. In testing mode, the actuators were always operated in closed loop load control from the load cells [9] - [10].

Secondary bending stresses caused by welding distortions were measured by strain gauges attached to the web plate about 10 mm from the stiffener weld toe. In this manner, the local nominal stress was obtained, disregarding the stress enhancement caused by the weldment. In general, the secondary bending stresses were found to be within 10-20 per cent of the nominal membrane stress in the web. These stresses were taken as an inherent feature of large scale welding fabrication, and hence disregarded in the analysis of S-N data as well as in the fracture mechanics model.

Test procedure

A block program was designed to resemble the general shape of stress spectra for marine structures, cf. Fig. 3. The block levels were chosen such that the peak load would occur once in each period, and each period would have to be repeated at least 300 times in order to give a Miner-Palmgren sum of unity. Thus, the loading could be assumed to be stationary.

In order to avoid excessive testing duration, the stress spectrum was truncated in the lower end. For the stiffener details the cut-off levels corresponded to constant amplitude endurances slightly below the classical fatigue limit at $2 \cdot 10^6$ cycles.

The stress blocks within each period were ordered in an ascending/descending sequence with a constant mean stress, cf. Fig. 4. One period of blocks contained about 6000 cycles. The details of the test spectrum are given in (6, 7). Only beam bending stresses were considered, i.e. shear stresses in the web were disregarded.

During testing, fatigue cracks developed at various locations in the plate girders. When reaching through thickness lengths, the cracks were repaired by welding and testing was resumed, thus enabling other cracks to develop further.

The welds were periodically checked for crack initiation by the magnaflux method. When cracks were detected, through thickness crack growth was monitored by a high-frequency, alternating current potential drop system.

Due to the variable amplitude loading, beachmarks were left on the crack surfaces. At the end of testing, the crack growth measurements were checked against the surface markings.

Crack initiation and growth

Fracture surface examinations showed that multiple cracks developed along the stiffener welds during the first stage of crack growth, i.e. fatigue cracks were initiating at various sites along the weld toe before joining into one single larger crack (crack coalescence). Typically crack coalescence occured at a crack depth of 5 mm, or 25 per cent of the plate thickness.

In several cases multiple cracks were detected at both sides of a stiffener detail. Generally through-thickness crack growth occured for one of these cracks only, while the crack on the opposite side of the stiffener was arrested.

A crack causing failure at a stiffener weld would go through three stages of growth as depicted in Fig. 5. In Stage 1 a semi-elliptical surface crack generated from multiple crack initiation was growing through the thickness of the web plate. Once the crack front had penetrated the web plate, the crack changed into a two-ended through crack. The transition after web plate penetration into Stage 2 occured within a small number of cycles.

In Stage 3 after the front of the two-ended crack had grown through the thickness of the tension flange, the crack grew as a three-ended crack across the flange and in the web.

In all the cases the crack followed the stiffener weld toe, indicating the bending stress to be the driving force for crack growth.

In order to continue testing, cracks were repaired by welding before the flange was completely severed. At this stage, the through thickness crack size in the

flange was in the range 100-150 mm. The crack growth rate observed at this stage indicated that the remaining fatigue life of the girders was negligible.

Under this assumption, about 90 per cent of the total fatigue life of the plate girders was consumed in Stage 1, i.e. the part-through crack growth stage. Stages 2 and 3 accounted for about 8 and 2 per cent respectively, cf. Fig. 5.

In a similar investigation on smaller scale plate girders, Fisher et al. (9) found that about 15 and 5 per cent of the total fatigue life were consumed in Stages 2 and 3 respectively. This discrepancy may be explained by size effects. A through thickness crack in a large specimen will be larger than in a geometrically similar small specimen, and the crack growth rate at this stage will be correspondingly greater. In the tests by Fisher et al., the plate thickness was 6.3 mm, as compared to 20 mm in the tests reported here.

FRACTURE MECHANICS ANALYSIS

Crack growth model

As observed by Signes et al. (10) and Watkinson et al.(11), the fatigue life of welded joints consists mainly of crack growth from pre-existing crack-like defects in the weld toe region. In the present study only the crack growth stage was considered, i.e. a possible crack initiation stage was neglected.

As observed in the tests, about 90 per cent of the total number of cycles to failure were consumed in through-thickness crack growth of the web plate (Stage 1). Hence only this stage of crack growth was considered in the analysis.

An in-house computer program LIFE as described by Engesvik and Moan (12) was used for the fracture mechanics calculations. Crack growth was assumed to follow the Paris-Erdogan type crack growth law

$$\frac{da}{dN} = C(\Delta K)^m \quad \ldots\ldots\ldots \qquad (1)$$

$$C = 5.36 \cdot 10^{-12} \quad [\mathrm{MPam}^{\frac{1}{2}},\ \mathrm{m}]$$

$$m = 3.0$$

These values fall within the scatterband of crack growth data for various structural steels (13), and are recommeded for fracture mechanics analysis of crack growth in welded steel structures (3).

The stress intensity factor was calculated by an influence function method, assuming the following form,

$$K = S\sqrt{\pi a}\ F_S\ F_T\ F_W\ F_E\ F_G \quad \ldots\ldots \qquad (2)$$

where

F_S - free surface correction factor
F_T - finite thickness correction factor
F_W - finite width correction factor
F_E - ellipticity correction factor
F_G - stress gradient correction factor

The correction factors F_S to F_E were expressed by parametric formulae taken from the literature.

This stress intensity factor calculation procedure requires that the crack ellipticity is entered as an input parameter (12). The ellipticity was taken from crack shape measurements on the fracture surfaces of the stiffener welds. The crack shape data are shown in Fig. 6. A linear regression analysis of the data gave the following empirical relations,

$$\begin{aligned} 2c &= 2.79a + 0.1\ , && a < 5\ \text{mm} \\ 2c &= 3.75a + 0.8 && a \geq 5\ \text{mm} \end{aligned} \qquad (3)$$

The physical simulation thus simulated is one of multiple cracks initiated along the stiffener weld toe, growing independently of each other until coalescence on a common crack front at a = 5 mm. As will be noted, fatigue life at this stage has very nearly expired.

F_G was calculated from the stress distribution across the crack plane using a point-load model (12). The stress distribution was calculated by FEM using a two-dimensional model for the stiffener weld geometry.

The significant parameters in defining weld geometries for FEM analysis are shown in Fig. 7. The actual FEM analysis is carried out using a super-element technique, as shown for a cruciform joint in Fig. 8. With this method, only one FEM analysis is required for each geometry. With a given nominal stress, it is thus straight forward to model any weld geometry, provided the geometry is suitable for two-dimensional analysis.

The variable amplitude fatigue life was calculated by numerical integration, using the equivalent constant amplitude stress range approach. Thus, possible stress interaction and threshold effects were neglected.

As shown by the authors (14), in variable amplitude loading the equivalent constant amplitude stress range can be expressed as

$$\Delta S_{equ} = \left[\frac{\sum n_i \, (\Delta S_i)^m}{\sum n_i}\right]^{1/m} \qquad (4)$$

where

m - exponent of the Paris-Erdogan equation
n_i - number of cycles with stress range ΔS_i

Fracture mechanics analysis

It has been recognized that crack-like defects in the weld toe region is an inherent feature of welds produced by conventional welding processes (10, 11). These defects are non-metallic slag intrusions along the fusion line, formed when the metal is melted or pasty during welding. Typically the defect depths are in the range 0.05-0.4 mm, with a mean value of about 0.1 mm. A consequence of these findings is that the crack initiation stage is small, and can be neglected in fatigue life calculations.

In Fig. 9 computed crack growth curves for a range of initial crack sizes are compared to the experimental data. The experimental data were obtained from 6 different cracks with equivalent stress ranges 106-115 MPa. The data are plotted on the basis of normalized stresses, i.e. for a given crack depth the corresponding number of cycles N_o was adjusted according to

$$N = N_o \left(\frac{\Delta S_o}{\Delta S}\right)^m \quad \ldots\ldots \qquad (5)$$

where ΔS_o is a reference equivalent stress range.

It is noted that the experimental observations fall well within the scatterband given by an assumed range of initial crack depths. Moreover, an initial crack

depth of 0.1 mm seems to model the average crack growth behaviour as well as the through-thickness fatigue life with good consistency.

TABLE 1 - Results from Fatigue Life Computation

Crack depth a [mm]	No. of cycles N	Fraction of total life [%]	Residual life [%]
0.1	0	0	100
1.0	865.341	44.1	55.9
3.0	1.369.544	59.9	30.1
5.0	1.629.775	83.1	16.9
10.0	1.853.524	94.6	5.4
15.0	1.928.931	98.4	1.6
20.0	1.960.396	100.0	0

In Table 1 are shown the computed number of cycles at various crack depths during through thickness crack growth. It is noted that at a crack depth of 3 mm, i.e. 15 per cent of the plate thickness, about 70 per cent of the through-thickness fatigue life has expired. At a crack depth of half the plate thickness, only 5 per cent of the part-through fatigue life is remaining.

DISCUSSION

Methods for crack detection and sizing are essential prerequisites if rational in-service inspection and repair criteria are to be formulated. In Fig. 10 is shown the probability of detection of part-through cracks with ultrasonic and radiographic inspection methods as assessed by Harris (15). Assuming that a 90 per cent crack detection probability is desired for the purpose of determining if the structure should remain in service, only cracks larger than 6.3 mm and 7.8 mm would be detected with ultrasonic and radiographic inspection

respectively. Comparing these values with the crack sizes given in Table 1, it is noted that 90 per cent of the part-through crack growth life has been consumed by the time a crack may be detected with a 90 per cent reliability.

In the discussion, remaining fatigue life in Stages 2 and 3 has been disregarded, cf. Fig. 5. As noted from the experimental data, this amounted to about 10 per cent of the total fatigue life of the girders. However, this stage of crack growth is subject to size effects which for a given geometry could reduce the remaining life even further. Moreover, in real structures the allowable crack length will be limited by fracture toughness criteria. It is not uncommon in welds to find lower bound toughnesses corresponding to allowable crack lengths of the order of 20 mm under design conditions. This indicates that Stages 2 and 3 should be taken into consideration in fatigue analysis only after close scrutiny of the criteria governing final failure.

CONCLUSIONS

Large scale welded girders with 20 mm plate thickness were fatigue tested in the as-welded condition. Crack growth from transverse stiffeners was monitored. A fracture mechanics model was established, based on a detailed stress analysis of the welds. The following may be concluded form the study.

- In most cases, fatigue cracks were initiated at several locations along the toe of the stiffener welds. At a crack depth of about 5 mm, the initial cracks coalesced into one long surface crack. At this stage, about 83 per cent of the through thickness fatigue life had expired.

- If total fatigue life is taken as life to complete severance of the girder flange, the stage of crack growth to through thickness of the web accounted for about 90 per cent of the total life.

- On the basis of a normalized stress, crack growth data from different cracks could be unified within a common scatter-band.

- The fracture mechanics model gave results in good agreement with the experimental data, assuming crack growth from an initial defect depth of 0.1 mm. A sen-

sitivity analysis showed that the observed scatter in test data could be accounted for by assuming the initial defect size to vary within a very small range around this value.

- Using established data for the probability of crack detection by industrial inspection methods, the crack growth data indicate that a crack size with a 90 per cent probability of detection corresponds to a stage where 90 per cent of the useful fatigue life has expired.

- The fracture mechanics model is capable of taking into account various weld geometries and crack shapes, and provides a tool for assessment of residual fatigue life of plated structures with crack-like defects.

ACKNOWLEDGEMENT

This work has been carried out under "The National 5-years Research Program for Fatigue of Offshore Steel Structures" and the "Research Program for Marine Structures". Financial support is gratefully acknowledged from The Royal Norwegian Council for Scientific and Technical Research, The Norwegian Petroleum Directorate, Kværner Engineering, Norsk Hydro, Phillips Petroleum Company Norway, and Statoil.

REFERENCES

(1) "Design recommendations for cyclic loaded welded steel structures", Welding in the World, 20 No. 7/8, pp. 153-165 (Doc. IIW-693-81), 1982.

(2) "Offshore Installations: Guidance on design and construction", UK Department of Energy, 1977.

(3) "Rules for the design, construction and inspection of offshore structures", Det norske Veritas, 1977.

(4) Gurney, T.R. and Maddox, S.J., "A Re-analysis of Fatigue Data for Welded Joints in Steel", The Welding Institute Report E/44/72, 1972.

(5) Smith, I.J. et al., "Assessment of Fracture Toughness Requirements for the Deck Structure of the Hutton Tension Leg Platform using Finite Elements and the CTOD Design Curve," OTC 4430, Offshore

Technology Conference, Houston, 1982.

(6) Eide, O.I., Berge, S., and Moan, T., "Fatigue Capacity of Large Scale Girders", OTC 5001, Offshore Technology Conference, Houston, 1985.

(7) Eide, O.I., Berge, S., and Moan, T., "The Effect of Welding Stresses in Fatigue of Large Scale Girder Models", Proc. Int. Conf. on Effects of Fabrication Related Stresses on Product Manufacture and Performance, Cambridge, 1985.

(8) Fisher, J.W., Frank, K.H., Hirt, M.A. and McNamee, B.M., "Effect of Weldments on the Fatigue Strength of Steel Beams", National Cooperative Highway Research Program Report No. 102, 1970.

(9) Fisher, J.W. et al., "Fatigue Strength of Steel Beams with Fillet Welded Stiffeners and Attachments", National Cooperative Highway Research Program Report No. 147, Lehigh University, Pennsylvania, 1974.

(10) Signes, E.G. et al., "Factors Affecting the Fatigue Strength of Welded High Strength Steels", British Welding Journ., March 1967.

(11) Watkinson, F. et al., "The Fatigue Strength of Welded Joints in High Strength Steels and Methods for its Improvement", Proc. Conf. on Fatigue of Welded Structures, Brighton, 1970.

(12) Engesvik, K. and Moan, T., "Probabilistic Analysis of the Uncertainty in Fatigue Capacity of Welded Joints", Engng. Fract. Mech., Vol. 8, No. 4, 1983.

(13) ECSC Conference on Steel in Marine Structures, Institut de Recherces de la Siderurgie Francaise, Paris, 1981.

(14) Eide, O.I. and Berge, S., "Cumulative Damage of Longitudinal Non-load Carrying Fillet Welds", Proc. Fatigue -84, The Second International Conference on Fatigue and Fatigue Thresholds, Birmingham, 1984.

(15) Harris, D.O., "An Analysis of the Probability of Pipe Rupture Cooling Loop at a Babcock and Wilcoc 177 Fuel Assembly Pressurized Water Reactor - Including the Effects of a Periodic Inspection", Report SAI.050.77-PA, Science Applications, La Jolla, Calif., 1977.

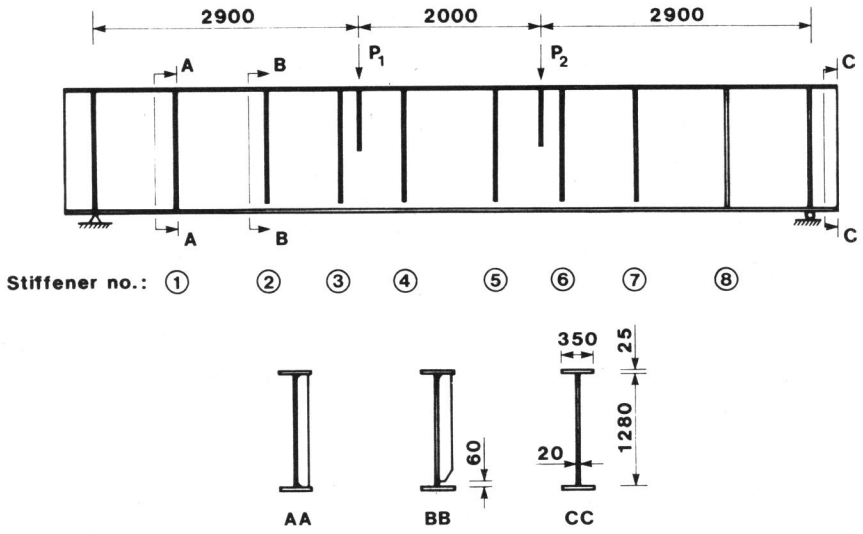

Figure 1 Specimen and loading

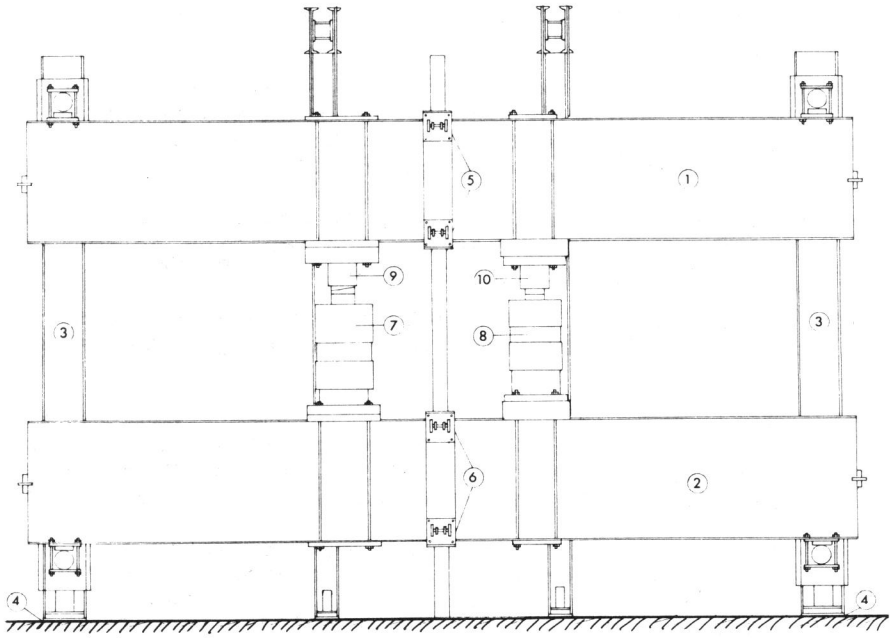

Figure 2 Test rig

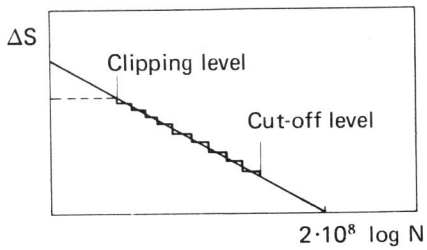

Figure 3

Stress spectrum typical for marine structures with block approximation, clipping level and cut-off level illustrated

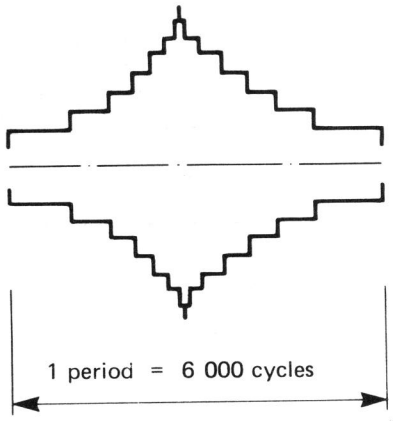

Figure 4 Block program sequence

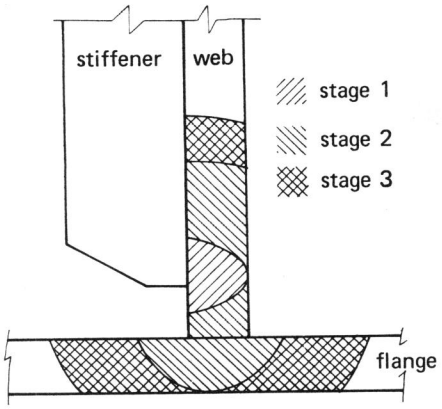

Figure 5 Stages of crack growth

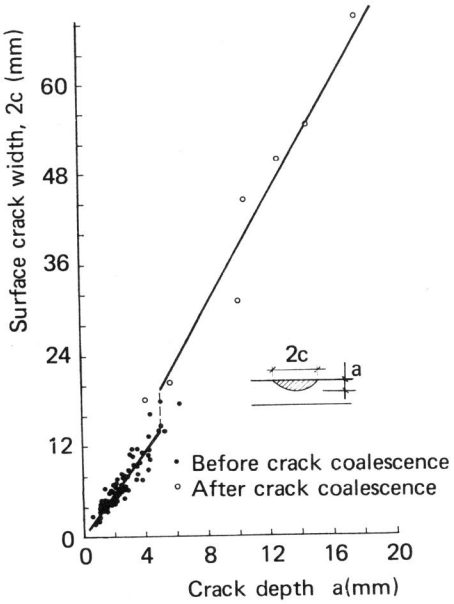

Figure 6 Crack shape data

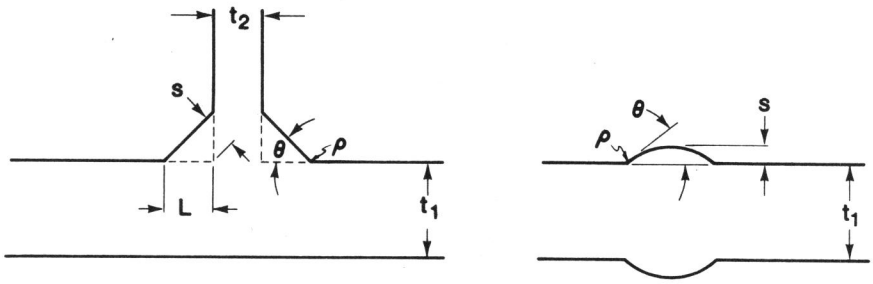

Figure 7 Definition of weld geometry parameters for FEM analyses

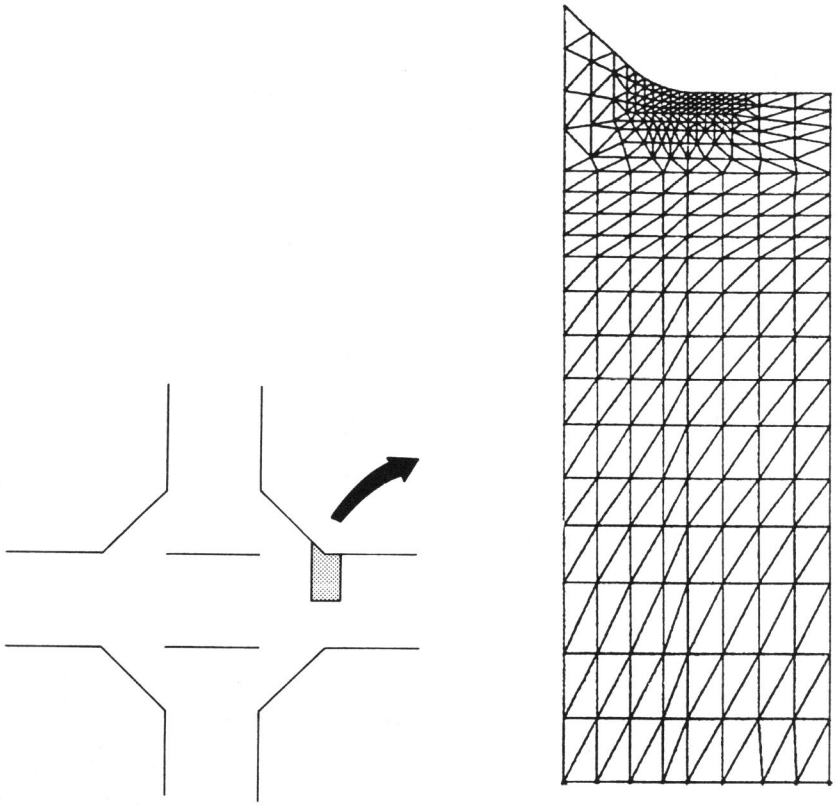

Figure 8 Typical FEM model applied in calculation of stress distribution along crack plane. Mesh is shown in substructure only.

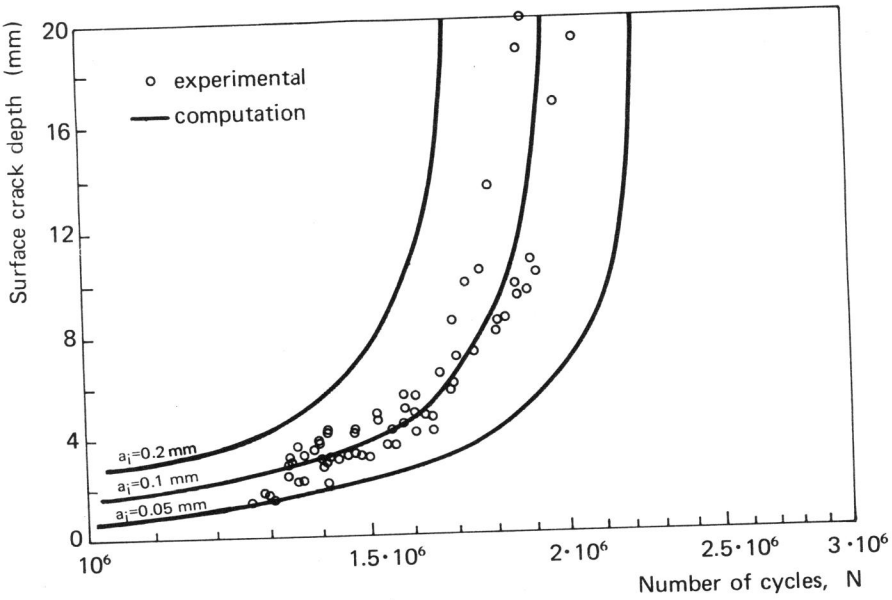

Figure 9 Comparison of computational and experimental results

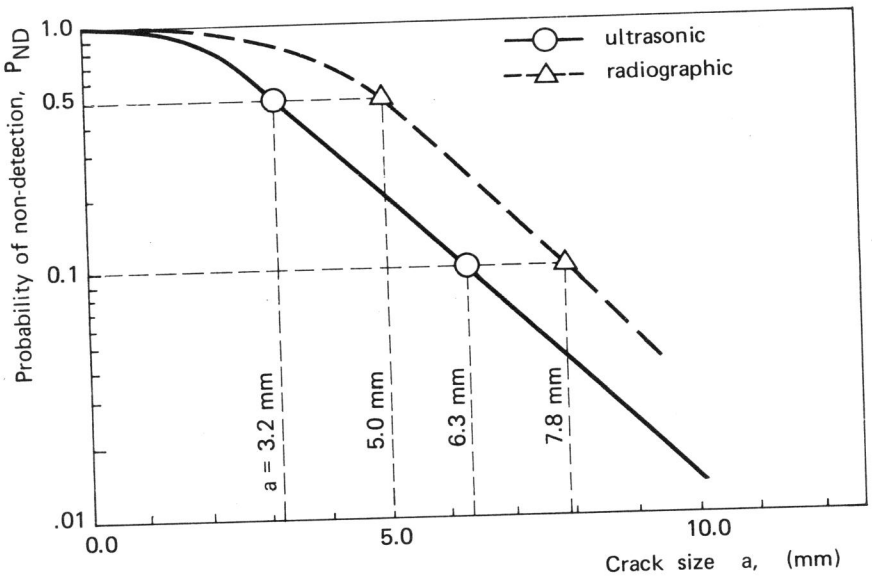

Figure 10 Probability of not detecting a crack by ultrasonic and radiographic inspection as a function of crack depth (15)